Journal of Russian Laser Research, Volume 22, Number 1, 2001

ON THE NEUTRON YIELD IN THE TWO-BEAM SCHEME OF LASER HEATING AND COMPRESSION OF SPHERICAL SHELL TARGETS WITH A LOW-DENSITY COATING

A. B. Iskakov,[1] I. G. Lebo,[2] V. B. Rozanov,[2] and V. F. Tishkin[1]

[1] *Institute of Mathematical Modeling, Russian Academy of Sciences, Miusskaya Pl. 4a, Moscow 125047, Russia*

[2] *P. N. Lebedev Physical Institute, Russian Academy of Sciences, Leninskii Pr. 53, Moscow 117924, Russia*

e-mail: lebo@sci.lpi.msk.su

Abstract

At the initial stage of development of large-scale multiple-beam laser facilities for the "ignition" of the fusion reaction, facilities with a small number of beams is expected to be created. Such facilities are characterized by poor symmetry of irradiation of spherical targets. We have shown that with appropriate design of the target and distribution of the radiation intensity in laser beams the attainment of a neutron yield of 10^{15}–10^{16} is possible even in two-side irradiation of the spherical targets.

1. Introduction

With the aim of demonstrating the "ignition" of thermonuclear targets, efforts are under way in the USA and France to create high-power multiple-beam neodimium-doped glass laser facilities with a pulse energy about 1–2 MJ [1]. Similar projects are also under development in Russia. It is generally believed that at the intermediate stage of creation of such plants it will be functional with a small number of beams (two, six, and so on). In this case, good symmetry of irradiation of the spherical targets is generally unattainable.

In this paper the results of two-dimensional (2D) numerical calculations of the heating and compression of spherical shell targets coated with a low-density absorber (e.g., with a foam) outside are presented. Such an absorber is necessary to avoid the regular refraction of the laser beams in the target corona (the spherical plasma flying apart plays the role of a "diverging lens," resulting in energy losses and creation of additional inhomogeneity of corona heating). It is also conceivable that the absorption of laser radiation in the porous structure will result in the symmetrization of the small-scale disturbances of the laser-radiation flux ("speckles"). In [2, 3], the impossibility of symmetrization of the large-scale inhomogeneity of the target irradiation (with a characteristic size of about the radius) arising from the design features of facilities with a small number of laser beams only at the expense of small-density layers was shown. The use of the special "relief" of the target for the hydrodynamic compensation of such an inhomogeneity was also proposed. The application of the laser with a smaller intensity of radiation in the center of the beam as compared to that at its edge was discussed in [4]. In this case, spherically symmetric heating of the target can be provided for the motionless plasma even with two beams.

In the present paper, the self-consistent solution for the heating and compression of the shell targets by such laser beams was obtained using the 2D numerical calculations.

Translated from a manuscript submitted November 27, 2000.

1071-2836/01/2201-0082$25.00

2. Brief Description of the "ATLANT-C" 2D Gasdynamic Program

All calculations were carried out using the "ATLANT-C" 2D gasdynamic program decribing the medium in Lagrangian coordinates. This program is destined for the simulation of the flows of gas and laser plasma in a broad range of initial conditions. The three-temperature model of gas dynamics in cylindrical geometry for a single liquid is used in the program. The processes of ionization and recombination as well as the propagation of laser radiation in the geometric optics approximation are taken into account in the program apart from those of the 2D gas dynamics and three-temperature heat conduction.

The set of equations solved with the program is presented below:

$$\frac{d\rho}{dt} = -\rho\vec{\nabla}\vec{v},$$

$$\rho\frac{d\vec{v}}{dt} = -\vec{\nabla}(Z_i P_E + P_I + P_R),$$

$$Z_i\rho\frac{dE_E}{dt} = -Z_i P_E\vec{\nabla}\vec{v} + \vec{\nabla}(k_E\vec{\nabla}T_E) - Q_{EI} - Q_{ER} - R_{RAD}(\rho, T_E) + \vec{\nabla}\vec{q},$$

$$\rho\frac{dE_I}{dt} = -P_I\vec{\nabla}\vec{v} + \vec{\nabla}(k_I\vec{\nabla}T_I) + Q_{EI},$$

$$\rho\frac{dE_R}{dt} = -P_R\vec{\nabla}\vec{v} + \vec{\nabla}(k_R\vec{\nabla}T_R) + Q_{ER},$$

$$P_E = P_E(\rho, T_E),\ P_I = P_I(\rho, T_I),\ P_R = P_R(\rho, T_R),$$

$$E_E = E_E(\rho, T_E),\ E_I = E_I(\rho, T_I),\ E_R = E_R(\rho, T_R),$$

$$Q_{EI} = Q_{0EI}\frac{T_E - T_I}{T_E^{3/2}}Z_i\rho^2;\ Q_{ER} = Q_{0ER}\frac{T_E - T_R}{\sqrt{T_E}}Z_i\rho^2,$$

$$\frac{dZ_i}{dt} = Z_i[\varphi_1(\rho, T_E, Z_i) - \varphi_2(\rho, T_E, Z_i) - \varphi_3(\rho, T_E, Z_i)],$$

$$\left(\vec{\nabla}, \frac{\vec{k}}{|\vec{k}|}\right)\vec{q} = \frac{|\vec{q}|}{n}\left[\vec{\nabla}n - \frac{\vec{k}}{|\vec{k}|}\left(\frac{\vec{k}}{|\vec{k}|}, \vec{\nabla}n\right)\right] - \kappa(\rho, T_E)\vec{q}.$$

Here, ρ is the density; v is the velocity; Z_i is the effective degree of ionization; E_E, E_I, and E_R are the internal energies of electrons, ions, and photons referred to the unit volume; P_E, P_I, P_R,T_E, T_I, T_R,k_E, k_I, and k_R are the pressures, temperatures, and coefficients of thermal conductivity for the electron, ion, and radiation plasma components; Q_{EI} and Q_{ER} are the energy-exchange rates between the components; R_{RAD} are the radiation losses; $\vec{q}$ is the laser-radiation flux; κ is the absorption factor of laser radiation; $\vec{k}$ is the wave vector.

To increase the stability of the Lagrangian difference meshes, the special difference scheme is used in the algorithm described. In this scheme, the number of nodes of the difference mesh with preset thermodynamic variables is higher than that of the nodes with preset coordinates and velocities. Two versions of such a difference scheme are presented in Fig. 1. In version (a) the Lagrangian cell is divided into four parts by the diagonals. This allows one to set the thermodynamic variables (pressure and internal energies) in the centers of triangles, i.e., to increase the number of thermodynamic variables by a factor of four. Partition of the Lagrangian cell into twelve parts is possible (see Fig. 1b). This permits the number of thermodynamic variables and, respectively, the "elasticity" of the Lagrangian cell to be increased. The difference scheme with partitioning of the cell into twelve parts was used in the calculations discussed. A detailed description of this approach can be found in [5].

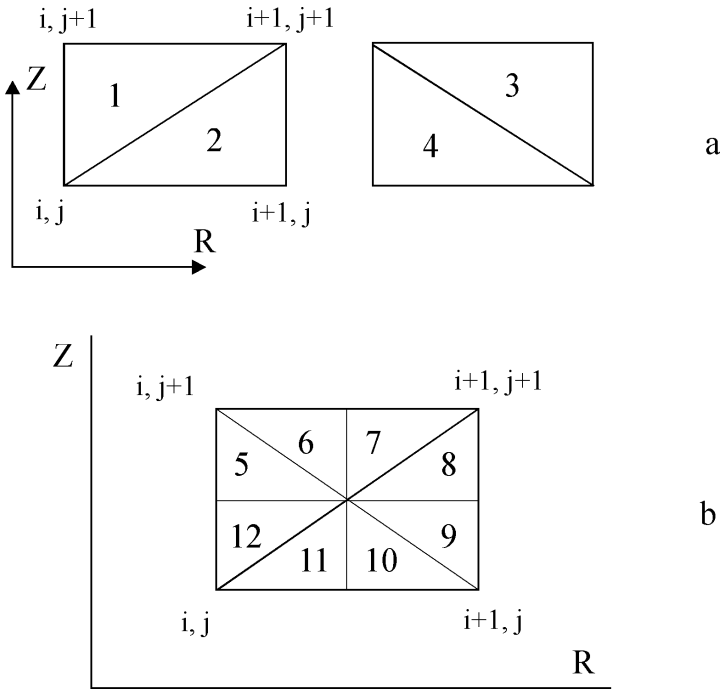

Fig. 1. Possible versions of partitioning of the tetragonal Lagrangian cell to increase the number of thermodynamic variables. The versions shown produce four (a) and twelve (b) thermodynamic variables per one cell.

The "ATLANT-C" permits simulation of the propagation of the laser radiation in plasma using the algorithm of beam propagation with account of the refraction and effects of thermal self-focusing. However, in the calculations presented, propagation of the laser beams strictly along the symmetry axis and absorption through the mechanism of inverse bremsstrahlung were suggested.

3. Calculation Results

The processes of heating and compression of the spherical targets under the action of two laser beams were considered in the calculations. The beams were incident on the target along the symmetry axis from the opposite sides. The beams of the neodymium-doped glass laser were characterized by a wavelength of 1.06 μm, total power of two beams of 100 kJ, and pulse duration of 3 ns. The pulse shape was that of a right triangle (see Fig. 2c).The laser-radiation flux was built up linearly in time until the instant of 3 ns. To provide symmetry of irradiation, the radial distribution of the laser-radiation flux was set in the following form [4]: $q_L = q_1(t) \cdot q_2(r)$. Here, $q_1(t)$ is the time dependence of the laser-radiation flux, $q_2(r) = C/\sqrt{1-(r/R_f)^2}$, r is the distance from the axis, R_f is the initial radius of the target, and C is the normalization constant. The latter was chosen to obtain a total energy of 50 kJ in one beam.

Two types of spherical shell targets were considered, namely, gas-filled and cryogenic targets. The latter consisted of shells with deuterium-tritium (DT) ice frozen onto the inner surface. In both cases, the shell was covered with a low-density layer outside. A mean density of about 1 mg/cm^3 was attained using the foamlike material. Such a layer can improve the symmetry of the target heating owing to the characteristic features of interaction of the laser radiation with the foam [6]. In this case, the absorption of radiation is independent of the angle of incidence, and the regular reflection and refraction as well as the energy losses due to the outward-directed plasma flows are nearly absent. Figure 2 shows the designs of such shell targets

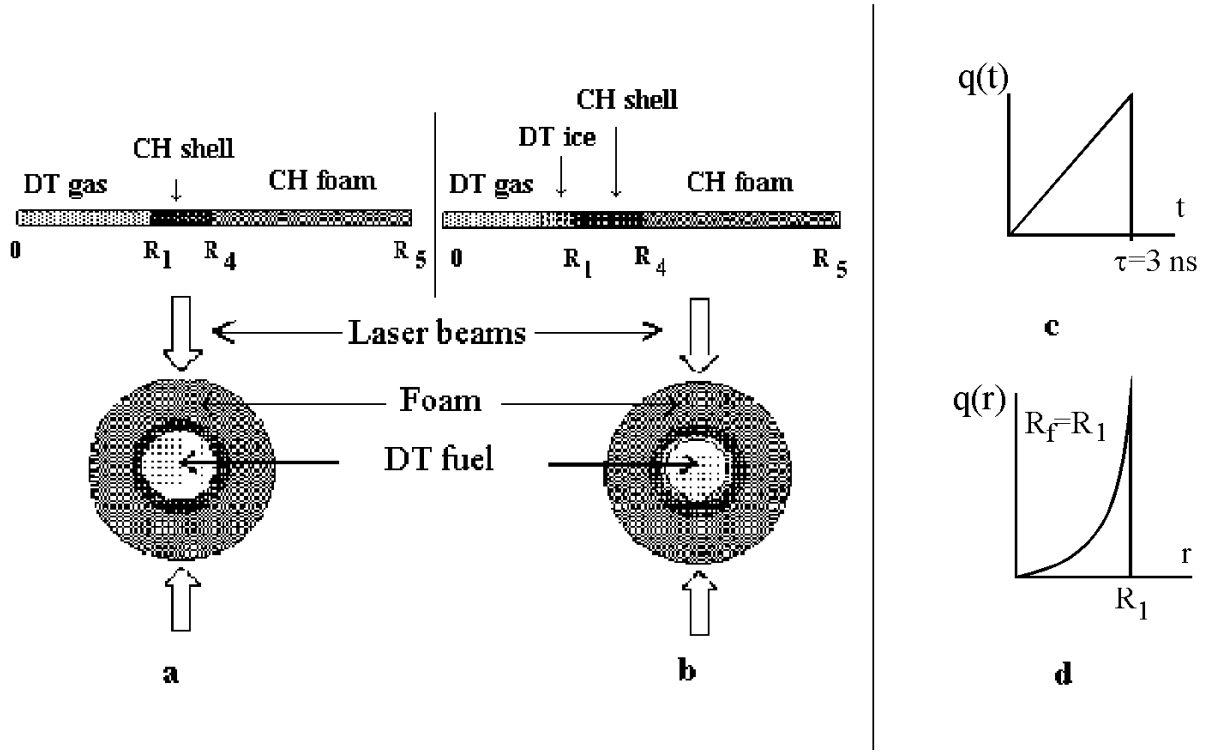

Fig. 2. Designs of the gas-filled (a) and cryogenic (b) targets as well as the temporary form of the laser pulse (c) and transversal distribution of the intensity of radiation in a single beam (d).

(a, b), the shape of the laser pulse (c), and the transversal distribution of the intensity of the laser beam (d).

The results of parameter optimization of the gas-filled targets for fixed parameters of the laser pulse are presented below. The scheme of such an optimization was proposed in [7].

In the first set of calculations, the radius of the shell and that of the whole target were fixed ($R_1 = 900$ μm, $R_5 = 1540$ μm), with $R_f = R_5$, while the thickness of the working shell (in other words, its mass) was varied. The results of calculations are presented in Fig. 3. The time of the target compression (collapse), t_{col}, decreases as the shell mass (M_{shell}) decreases. In the case where the thickness of the shell was 10 μm ($M_{\text{shell}} = 0.1$ mg), the time of collapse was 3.3 ns, i.e., it was matched to the duration of the laser pulse.

In the second set of calculations, the optimum mass of the fuel was chosen. In this case, the thickness of the working target was chosen to be 10 μm and the initial density of the DT gas mixture was varied. Figure 4 shows the dependence of the neutron yield on the initial mass of the DT mixture. From Fig. 4 we note that the optimum value of the neutron yield (about $2 \cdot 10^{15}$) is achieved at an initial gas density of 0.5 mg/cm^3. The preliminary calculations were performed for the cryogenic target. The neutron yield increases in this case. For example, at a fixed mass of the fuel of 2 μg the neutron yield increases by nearly one order of magnitude as compared to the gas-filled target (the experimental points for the cryogenic target are denoted by crosses in Fig. 4).

One should note that the optimum values of the fuel mass in the gas-filled targets are inconsistent with those for the cryogenic targets. Moreover, the neutron yield for the cryogenic targets also depends on the initial density of the residual gas. For these reasons, the optimization problem becomes at least a two-parameter one. The results of such a complete optimization will be presented in a subsequent paper.

Figure 5 shows the results of 2D simulation of the gas-filled target with optimum thickness of the shell

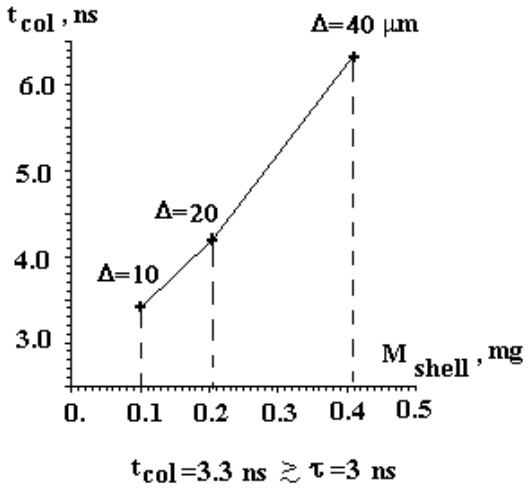

Fig. 3. Dependence of the compression time of the target on the mass of the working shell. The symbol Δ designates the corresponding thickness of the polyethylene shell. The optimum mass corresponds to a target with thickness of the shell 10 μm. The parameter $R_1 = 900$ μm.

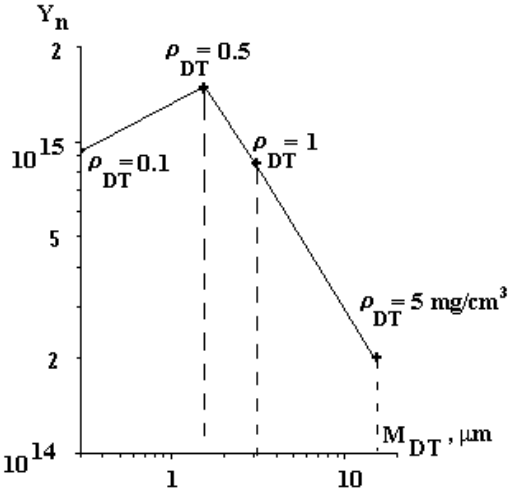

Fig. 4. Dependence of the neutron yield on the initial mass of the deuterium-tritium fuel. Optimum density of the DT gas mixture is 0.5 mg/cm^3.

(10 μm) and optimum fuel mass. The figure corresponds to the instant of maximum compression, $t = 3.28$ ns. In Fig. 5a, the density distributions along the axis (solid line) and at the angle $\theta = \pi/2$ are presented as a function of the distance from the target center. The maximum density of the fuel reaches up to 30–50 g/cm^3, while the maximum ion temperature is as much as 5–7 keV. The neutron yield was about 10^{15}. Figure 6 shows the distributions of the density and temperature at the time moment of 3.5 ns when the target has already completely collapsed after impact against the center. Note that, in spite of the acceleration of the shell towards the center having spherical symmetry, we failed to accomplish the ideal spherically symmetrical compression. In Fig. 7 the distributions of the plasma speed along the axis at the angle $\theta = \pi/2$ are presented as a function of the distance from the target center as well as the shape of the laser target at the time moment

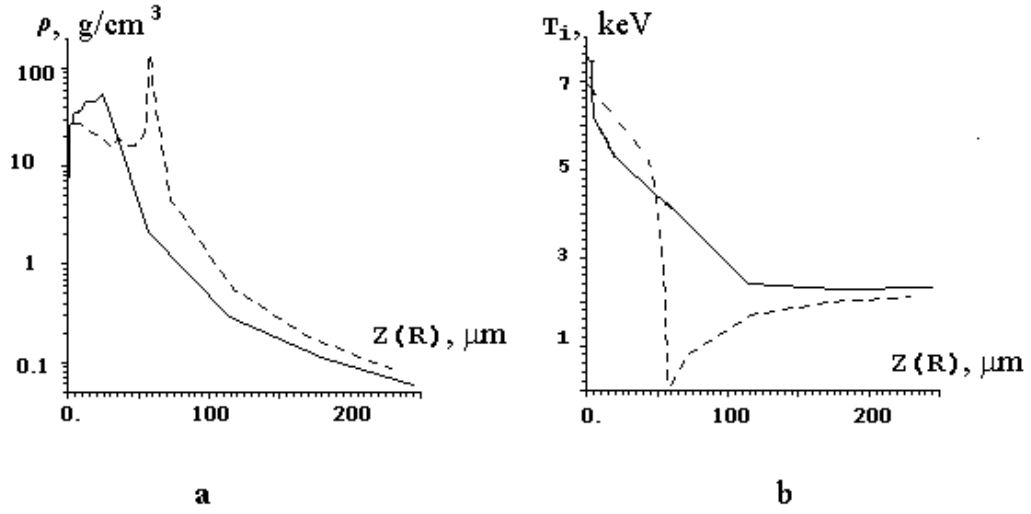

Fig. 5. Distributions of the density (a) and ion temperature (b) along the 0Z axis (solid lines) and at the angle $\theta = \pi/2$ at the time moment of 3.28 ns (instant of the maximum compression).

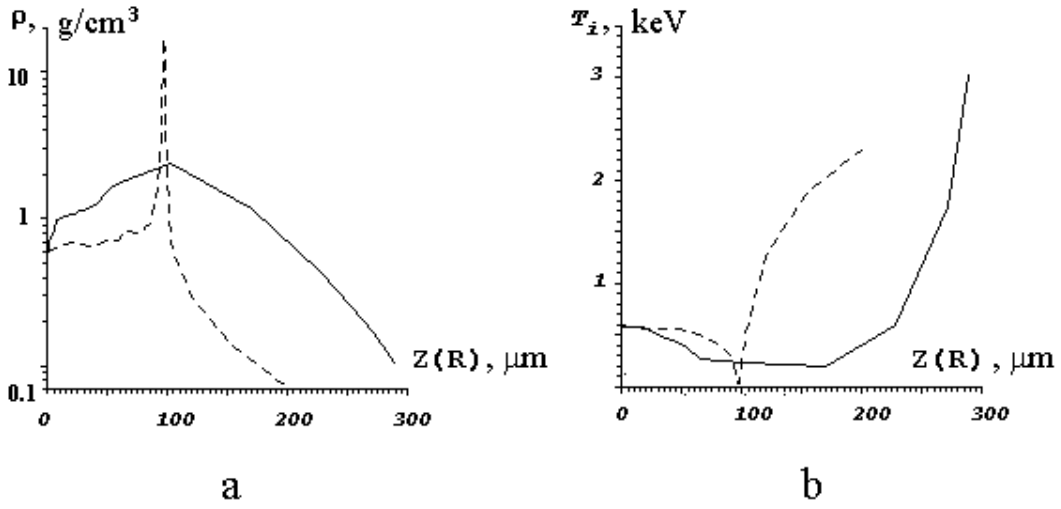

Fig. 6. Distributions of the density (a) and ion temperature (b) along the 0Z axis (solid lines) and at the angle $\theta = \pi/2$ at the time moment of 3.5 ns.

$t = 3.5$ ns.

4. Discussion

We emphasize that in our calculations up to 30% of the laser energy is not absorbed due to the fast compression of the working target. This energy passes by the target in the plasma corona even in the case where the reflection of the laser beams is neglected. One of the possible methods of "interception" of the radiation transmitted is the introduction of the ring from the dense material into the design of the target. This ring resides in the equatorial plane of the target and has an inner radius equal to the radius of the

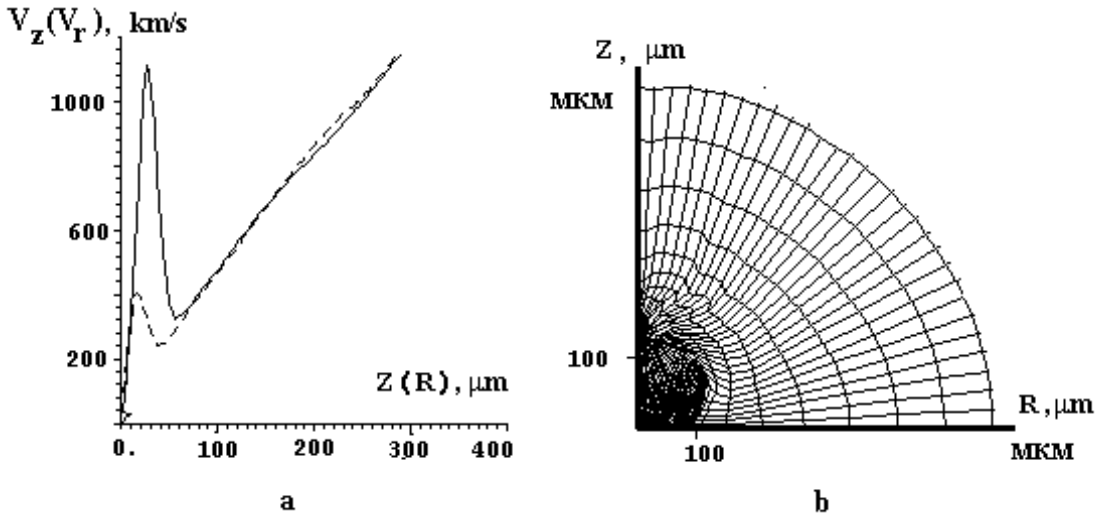

Fig. 7. Distributions of the speed components V_z at $\theta = 0$ (solid curve) and V_r at $\theta = \pi/2$ (dashed line) at the time moment of 3.5 ns (a) as well as the shape of the target (Lagrangian mesh) at the time moment of 3.5 ns (b).

working target, while its outer diameter equals the radius of the low-density coating ("Saturnian ring"). Such an approach was employed, in particular, in the experiments on the "Novietta" facility in USA (Lawrence Livermore National Laboratory).

The second possibility to increase the portion of the energy absorbed and, correspondingly, the neutron yield consists in decreasing the diameter of the focal spot during the compression of the working target. This can be achieved, for example, by the displacement of the laser focus ("zooming").

The use of a working shell with variation of its thickness according to the special "relief" was proposed in [2, 3] to improve the symmetry of compression and increase the neutron yield.

The parameters of the fuel compression can also be improved by changing to cryogenic targets.

5. Conclusions

The results of the two-dimensional numerical calculations presented show the possibility of a relatively high neutron yield (10^{15} at a laser energy about 100 kJ) in the case of a special profile of the laser irradiation of the targets with the low-density coating. The use of cryogenic targets with "relief" of the working shell and the steps taken to increase the portion of the absorbed laser energy listed above should produce an increase in the neutron yield by one further order of magnitude.

It is our opinion that such experiments show considerable promise at the intermediate stage of creation of facilities for laser-induced thermonuclear fusion.

Acknowledgments

This work was supported in part by the Russian Foundation for Basic Research (under Project No. 00-02-17188).

References

1. Book of Abstracts of the First International Conference on Inertial Fusion and Applications (IFSA'99) (University Bordeaux 1, Bordeaux, France, September 1999).
2. I. G. Lebo, V. B. Rozanov, and V. F. Tishkin, *Laser and Particle Beams*, **12**, 361 (1994).
3. I. G. Lebo, I. V. Popov, V. B. Rozanov, and V. F. Tishkin, *Quantum Electronics*, **12**, 1226 (1995).
4. S. Yu. Gus'kov, N. V. Zmitrenko, V. B. Rozanov, and R. V. Stepanov, in: *Proceedings of the XXIV Europian Conference on Laser Interaction with Matter* (Prague, Czech Republic, June 2000), to be published.
5. A. B. Iskakov, I. G. Lebo, and V. F. Tishkin, *J. Russ. Laser Res.*, **21**, 247 (2000).
6. G. A. Vergunova, A. I. Gromov, S. Yu. Gus'kov, et al., *J. Russ. Laser Res.*, **21**, 335 (2000).
7. S. Yu. Gus'kov, A. E. Danilov, Yu. A. Zakharenkov, et al., *Kvantovaya Élektron.*, **14**, 2288 (1987).